SF2A 2011
G. Alecian, K. Belkacem, R. Samadi and D. Valls-Gabaud (eds)

THE STAR FORMATION RATE DENSITY AND DUST ATTENUATION EVOLUTION OVER 12 GYR WITH THE VVDS SURVEYS

O. Cucciati[1], L. Tresse[1], O. Ilbert[1] and O. Le Fèvre[1]

Abstract.
We investigate the cosmic star formation rate density (SFRD) over ∼12 Gyr ($0.05 \leq z \leq 4.5$), combining the VVDS Deep ($17.5 \leq I_{AB} \leq 24.0$) and Ultra-Deep ($23.00 \leq i'_{AB} \leq 24.75$) surveys. We obtain a single homogeneous spectroscopic redshift sample, totalizing about 11000 galaxies. We estimate the rest-frame FUV luminosity function (LF) and luminosity density (LD), extract the dust attenuation of the FUV radiation using SED fitting, and derive the dust-corrected SFRD. We find a constant and flat faint-end slope alpha in the FUV LF at $z < 1.7$. The absolute magnitude M^*_{FUV} brightens in the entire range $0 < z < 4.5$, and at $z > 2$ it is on average brighter than in the literature, while ϕ^* is smaller. Our total LD shows a robust peak at $z \simeq 2$, and the SFRD history peaks as well at $z \simeq 2$. This peak is produced by the decreasing contribution at $z < 2$ of galaxies with $-21.5 \leq M_{FUV} \leq -19.5$ mag. As times goes by, the total SFRD is dominated by fainter and fainter galaxies. Moreover, at $z > 2$ the SFRD is entirely shaped by the high specific SFR galaxies. The presence of a fast rise at $z > 2$ and of a clear peak at $z \simeq 2$ of the SFRD is compelling for models of galaxy formation. The mean dust attenuation A_{FUV} of the global galaxy population rises by 1 mag from $z = 4.5$ to $z = 2$, reaches its maximum at $z = 1$ ($A_{FUV} \simeq 2.2$ mag), and then decreases by 1.1 mag down to $z = 0$. The dust attenuation maximum is reached 2 Gyr after the SFRD peak, implying a contribution from the intermediate-mass stars to the dust production at $z < 2$.

Keywords: cosmology: observations, galaxies: evolution, luminosity function, high-redshift - star formation

1 Data analysis

This work is extensively described in Cucciati et al. (2011). We use ∼ 11000 galaxies with spectroscopic redshift within $0.05 < z \leq 4.50$ taken from the VVDS Deep ($17.5 \leq I_{AB} \leq 24.0$, ∼ 2100 arcmin^2) and Ultra-Deep ($23.00 \leq i'_{AB} \leq 24.75$, ∼ 500 arcmin^2) surveys (Le Fèvre et al. 2005 and Le Fèvre et al. in prep.). We use the available photometric data (the BVI with CFHT-12K camera, the $u^*g'r'i'z'$ with the MEGACAM camera and the JHK_s bands with the WIRCAM camera,) to derive the FUV-band intrinsic luminosities with a SED fitting technique (Algorithm for Luminosity Function, ALF, Ilbert et al. 2005). We choose the template library from Bruzual & Charlot (2003) modulated by the attenuation of the intrinsic stellar continuum, $A(\lambda) = k(\lambda)E(B-V)$, where $E(B-V)_{star}$ is the intrinsic colour excess of the stellar continuum of a galaxy, and $k(\lambda)$ is the starburst reddening curve in Calzetti et al. (2000).

In this work, we have primarily estimated the rest-frame FUV luminosity functions (LF) and densities (LD) to derive the SFRD history. The recent SFR is traced by the intrinsic non-ionising ultraviolet stellar continuum ($91.2 - 300$ nm) of galaxies. Within this UV range, the far UV radiation (FUV-150) is a better SFR indicator than the near UV radiation (NUV-250), because the NUV is contaminated by evolved stars, while the FUV is dominated by the radiation from new, massive, short-lived stars (see, e.g., Madau et al. 1998).

The galaxy luminosity function (LF) usually follows a Schechter (1976) function characterised by a break luminosity, L^*, a faint-end slope, α, and a normalisation density parameter, ϕ^*. We derive the FUV-band LF in 10 different redshift bins, using our code ALF that includes the non-parametric $1/V_{max}$, SWML, and C^+ and the parametric STY luminosity function estimators (see Appendixes in Ilbert et al. 2005, and references therein). Our LF parameters are estimated with data brighter than the LF bias limit. We compute the rest-frame FUV

[1] Laboratoire d'Astrophysique de Marseille (UMR 6110), CNRS-Université de Provence, 38 rue Frédéric Joliot-Curie, F-13388 Marseille Cedex 13, France

LFs using a unique merged catalogue which includes both the Deep and Ultra-Deep surveys, for a total covered magnitude range of $17.5 \leq I_{AB} \leq 24.75$. This way, we exploit both the large magnitude range covered by the Deep survey and the depth reached by the Ultra-Deep survey. This leads us to a robust determination of the LF shape and normalisation.

We derive the mean comoving luminosity density (LD) in each redshift bin as $\mathrm{LD} = \int_{\mathrm{L_{faint}}}^{\mathrm{L_{bright}}} \phi(\mathrm{L})\ \mathrm{L\ dL}$, where $\phi(L)$ is the luminosity function assuming a Schechter (1976) functional form. We set $L_{faint} = 10^{15}$ W Hz^{-1} and $L_{bright} = 10^{25}$ W Hz^{-1} (corresponding to $M_{faint} \sim -3.4$ and $M_{bright} \sim -28.4$). Our LD uncertainties include errors from the STY LF fit, errors due to cosmic variance, Poisson noise, and errors associated to our weighting scheme.

We derived the FUV-band dust attenuation A_{FUV} in the following way. Our template SED fitting assigns to each galaxy a value of $E(B-V)_{star}$ chosen from a grid of five possible values $(0.1, 0.2, 0.3, 0.4, 0.5)$. In each studied redshift bin, we compute our resulting average $E(B-V)_{star}$. Then, to compute the mean A_{FUV} in each redshift bin, we follow the prescription in Calzetti et al. (2000), that is, $A(\lambda) = E(B-V)_{star}\ k(\lambda)$. Fig. 1 shows our A_{FUV} determination as a function of redshift.

We computed the dust corrected SFRD from our LD, transforming FUV fluxes into star formation rates with the FUV-SFR calibration of Madau et al. (1998), and correcting for the dust attenuation. We use the formula $\mathrm{SFRD}\ (z) = 1.4\,10^{-28}\,\mathrm{LD}_{FUV}(z)\,10^{0.4\ A_{FUV}(z)}$, where the SFRD is in $M_{\odot}\mathrm{yr}^{-1}\mathrm{Mpc}^{-3}$ units and the LD in erg s^{-1} Hz^{-1} Mpc^{-3}. Our SFRD is shown in Fig. 2 and Fig. 3.

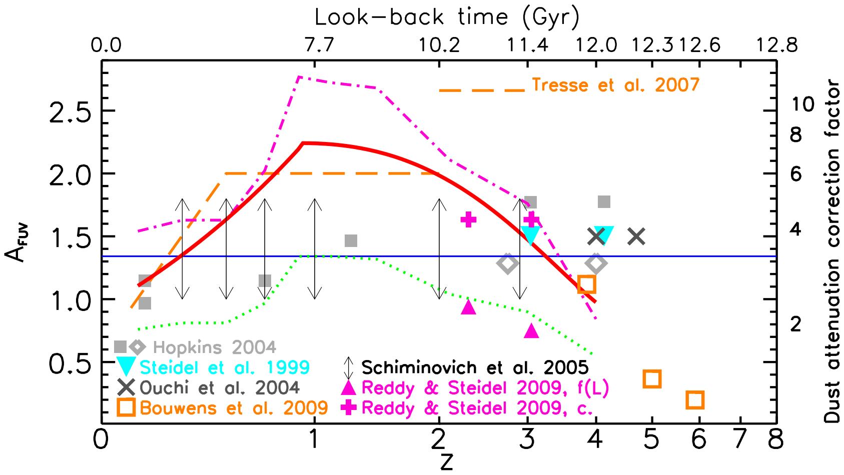

Fig. 1. Dust attenuation A_{FUV} in magnitudes as a function of redshift as found in this work (thick solid red curve). Magenta dot-dashed curve: average A_{FUV} determined in this work using the recipe in Meurer et al. (1999), based on the β slope. Green dotted curve: same as the dot-dashed one, but using the recipe in Cortese et al. (2006). Thin blue horizontal solid line: constant A_{FUV} computed with the Calzetti's law using one single typical value of $E(B-V)$ (=0.13). The right $y-axis$ shows the multiplicative factor to be applied to the observed luminosities, i.e., $10^{0.4A_{FUV}}$. All the other symbols represent dust attenuations found in literature, as indicated in the labels.

2 Results

Our result is an improvement with respect to the similar study of the FUV-band LD in Tresse et al. (2007), that was based on our first VVDS-Deep spectroscopic sample (Le Fèvre et al. 2005) and our UBVRI photometric sample (Le Fèvre et al. 2004). Our findings can be summarised as follows.

- We find a flat and constant faint-end slope in the FUV-band LF at $z < 1.7$ ($\alpha \sim 1$). We verified that this is unlikely to be the result of missing faint galaxies from our I-band selection, and that dust may have a role. At $z > 1.7$, we set α evolving with $(1+z)$, and this way it becomes as steep as -1.73 at $z \simeq 4$, consistent with values from deep photometric studies. M^{*}_{FUV} increases by ~ 4 mag from $z \sim 0$ to $z \sim 4.5$, while ϕ^{*} starts decreasing at $z > 0.7$ We find that at $z = 2, 3, 4$ our M^{*}_{FUV} is on average brighter than what has been found in previous works, and that ϕ^{*} is on average smaller, in particular at $z \sim 4$.

- We derived the evolution of the dust-attenuation in the FUV-band (A_{FUV}, see Fig. 1) in the range $0.05 < z \leq 4.5$, using a SED fitting method, in a consistent way from a single survey with a well controlled selection function. We find a continuous increase of A_{FUV} by ~ 1 mag from $z \sim 4.5$ to $z \sim 1$, then a decrease by the same amount from $z \sim 1$ to $z \sim 0$. This is the first time that the A_{FUV} evolution has been assessed homogeneously on such a broad redshift range.

- We traced the dust-corrected SFRD evolution over the past ~ 12 Gyr (see Fig. 2 and 3). Thanks to the homogeneity of our data over such a cosmic time, we have been able to unveil the presence of a peak at $z \sim 2$ in the cosmic SFR history. This peak is preceded by a rapid increase by a factor 6 from $z \sim 4.5$, then followed by a general decrease by a factor 12 to $z \sim 0$. We remark that the epoch of the peak of the dust-corrected SFRD ($z \sim 2$) does not coincide with that of the maximum of the dust attenuation evolution ($z \sim 1$), and that a peak at $z \sim 2$ is already present in the evolution of our LD.

- We find that as times goes by, the total SFRD is dominated by fainter and fainter galaxies. Moreover, the presence of a SFRD peak at $z \sim 2$ is due to a similar peak within the population of galaxies with $-21.5 \leq M_{FUV} \leq -19.5$, while the most extreme star-forming galaxies reaches their maximum activity at higher redshift (see Fig. 4). Finally, we find that the shape of the SFRD evolution at $z > 2$ is entirely due to galaxies with large specific SFR.

Our data therefore consistently show a peak in the LD and SFRD at $z \sim 2$, where the LF is well constrained. While the decrease in SFRD at $z > 2$ is not in question, the exact amplitude of this decrease remains to be investigated, as the faint end slope of the LF is still unconstrained even from our very deep spectroscopic survey.

3 Conclusions

The correct determination of the shape of the SFRD evolution is necessary to understand which physical processes mostly affect galaxy evolution. The SFRD is the result of the transformation of gas into stars and therefore requires a significant gas reservoir to sustain a strong star formation rate for a long time. A number of processes are expected to modify the gas reservoir hence the SFR, including the efficiency of star formation, cold accretion along the cosmic web filaments, mergers with gas-rich galaxies, stellar feedback, SN feedback blowing gas out from the galaxy core, AGN feedback, cosmic photoionizing radiation, or environment effects which may result in star formation quenching (e.g., among many others, White & Frenk 1991; Efstathiou 1992; Cole et al. 1994, 2000; Di Matteo et al. 2005; Baugh 2006; Cox et al. 2008; Dekel et al. 2009; de Ravel et al. 2009).The exact balance of these different processes along cosmic time will result in the observed SFRD. The SFRD peak that we find at $z \simeq 2$ is produced by intermediate luminosity galaxies, requiring that significant gas reservoirs still exist at this epoch and are probably replenished by cold accretion and wet mergers, while feedback or quenching processes are not yet strong enough to lower the SF. Knowing the SFRD, we may hope to identify the relative contribution of these different processes at different epochs.

Using simulations (semi-analytical galaxy evolution models, smoothed particle hydrodynamics simulation), several authors have attempted to reproduce the observed Cosmic Star Formation History with theoretical predictions (e.g. Baugh et al. 2005; Somerville et al. 2008; Hopkins et al. 2010; van de Voort et al. 2011). As a recent example, Weinmann et al. (2011) start from a standard model of galaxy evolution, and produce slightly different versions of it by tuning one or more ingredients at a time (such as star formation efficiency, stellar feedback, merger processes...). All of their models (see their Fig. 10) reproduce qualitatively the fast SFRD increase from $z \sim 0$ to $z \sim 1$, but at $z > 1$ the predicted SFRDs have different behaviours, showing growths at different rates, in some cases a plateau, and a more or less delayed decrease at higher redshifts. It is worth noticing that one of the models (where feedback has been tuned) predicts a sharp peak in the SFRD evolution at $z \sim 1.5$, qualitatively similar to the one that we find at $z \sim 2$. It is not the aim of this work to compare in details our findings with model predictions, and we will address this issue in more details in a future work. Here we want only to stress the importance of bringing strong observational constraints on the SFRD from a unique and homogeneous galaxy sample covering a large cosmic time of ~ 12 Gyr, which will need to be reproduced by next generation models.

Another remarkable finding of our work is that the peak of the dust and the SFR do not coincide, differently from what one could have naively thought in the case the dust is immediately released into the ISM a short time after supernova explosions of massive, short-lived stars which dominate the SFR. These two peaks are separated by ~ 2.5 Gyr, which is a long period if one considers that the dust production rate peak is below 1 Gyr for

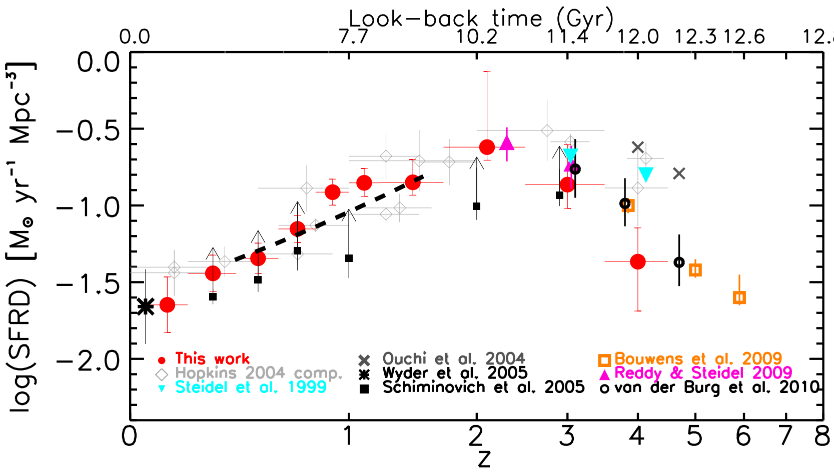

Fig. 2. Total dust-corrected UV-derived SFRDs as a function of redshift from the VVDS Deep+Ultra-Deep sample (red filled circles). Uncertainties are explained in the text. The black dashed line is the SFRD(z) implied from the stellar mass density in Ilbert et al. (2010). We overplot other results from the literature, as detailed in the labels. All SFRDs in this plot are derived using the FUV-band LDs converted into SFRD with the scaling relation from Madau et al. (1998). All data have been homogenised with the same IMF (Salpeter 1955).

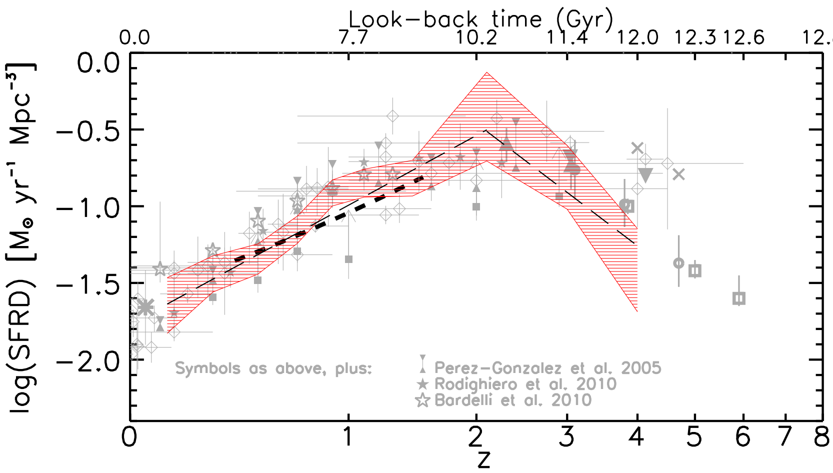

Fig. 3. Total dust-corrected UV-derived SFRDs as a function of redshift from the VVDS Deep+Ultra-Deep sample (red shaded area, corresponding to red circles and error bars in Fig. 2. The two long-dashed lines represent two fits to our SFRDs in the form $\propto (1+z)^{\beta}$ (see text for details). Gray points are from literature, derived from various SFR calibrators (UV, emission lines, IR, radio): they include the literature points as in Fig. 2, plus other works as in the labels.

SNII, but it is at 3-4Gyr for low-mass stars (see Dwek 1998). Nevertheless the dust reaches a sort of plateau from $z \sim 1.5$ (with a maximum at $z \sim 1$), i.e. 1 Gyr after the peak of the SFRD. Recently, Fukugita (2011) suggested that the dust must survive on much longer time scales than what has been previously thought and that half of the dust could be produced by SNII and the other half by low-mass (1-8 solar masses), long-lived stars. If we assume that the SNII dust production peaks very shortly after the SFRD peak, then the dust peak that we observe at $z \sim 1$ is likely due to intermediate-mass, long-lived stars producing their peak of dust on a delayed time. Surely, like in the case of the SFRD evolution, our findings about the general evolution of the FUV-band dust attenuation in such a broad cosmic epoch ($\sim$ 12 Gyr) will constitute an important reference for future models.

We thank S. Boissier for useful discussions. OC thanks V. Buat, D. Burgarella and L. Cortese for interesting conversations. This

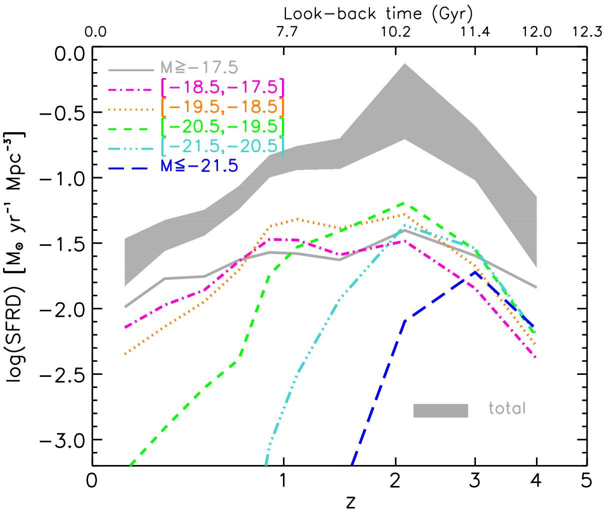

Fig. 4. The dust-corrected SFRD from galaxies in different FUV-band luminosity bins, as described in the labels. The background gray shaded area is the total SFRD.

work has been partially supported by the CNRS-INSU and its Programme National Cosmologie-Galaxies (France) and by INAF grant COFIN 2010.

References

Baugh, C. M. 2006, Reports on Progress in Physics, 69, 3101
Baugh, C. M., Lacey, C. G., Frenk, C. S., et al. 2005, MNRAS, 356, 1191
Bruzual, G. & Charlot, S. 2003, MNRAS, 344, 1000
Calzetti, D., Armus, L., Bohlin, R. C., et al. 2000, ApJ, 533, 682
Cole, S., Aragon-Salamanca, A., Frenk, C. S., Navarro, J. F., & Zepf, S. E. 1994, MNRAS, 271, 781
Cole, S., Lacey, C. G., Baugh, C. M., & Frenk, C. S. 2000, MNRAS, 319, 168
Cortese, L., Boselli, A., Buat, V., et al. 2006, ApJ, 637, 242
Cox, T. J., Jonsson, P., Somerville, R. S., Primack, J. R., & Dekel, A. 2008, MNRAS, 384, 386
Cucciati, O., Tresse, L., Ilbert, O., et al. 2011, ArXiv:1109.1005
de Ravel, L., Le Fèvre, O., Tresse, L., et al. 2009, A&A, 498, 379
Dekel, A., Birnboim, Y., Engel, G., et al. 2009, Nature, 457, 451
Di Matteo, T., Springel, V., & Hernquist, L. 2005, Nature, 433, 604
Dwek, E. 1998, ApJ, 501, 643
Efstathiou, G. 1992, MNRAS, 256, 43P
Fukugita, M. 2011, ArXiv e-prints
Hopkins, P. F., Younger, J. D., Hayward, C. C., Narayanan, D., & Hernquist, L. 2010, MNRAS, 402, 1693
Ilbert, O., Salvato, M., Le Floc'h, E., et al. 2010, ApJ, 709, 644
Ilbert, O., Tresse, L., Zucca, E., et al. 2005, A&A, 439, 863
Le Fèvre, O., Vettolani, G., Garilli, B., et al. 2005, A&A, 439, 845
Le Fèvre, O., Vettolani, G., Paltani, S., et al. 2004, A&A, 428, 1043
Madau, P., Pozzetti, L., & Dickinson, M. 1998, ApJ, 498, 106
Meurer, G. R., Heckman, T. M., & Calzetti, D. 1999, ApJ, 521, 64
Salpeter, E. E. 1955, ApJ, 121, 161
Schechter, P. 1976, ApJ, 203, 297
Somerville, R. S., Hopkins, P. F., Cox, T. J., Robertson, B. E., & Hernquist, L. 2008, MNRAS, 391, 481
Tresse, L., Ilbert, O., Zucca, E., et al. 2007, A&A, 472, 403
van de Voort, F., Schaye, J., Booth, C. M., & Dalla Vecchia, C. 2011, MNRAS, 415, 2782
Weinmann, S. M., Neistein, E., & Dekel, A. 2011, ArXiv:1103.3011
White, S. D. M. & Frenk, C. S. 1991, ApJ, 379, 52